

An Analytical Treatment of
Channel-Morphology Relations

GEOLOGICAL SURVEY PROFESSIONAL PAPER 1288



102.925

An Analytical Treatment of Channel-Morphology Relations

By W. R. OSTERKAMP, L. J. LANE, *and* G. R. FOSTER

GEOLOGICAL SURVEY PROFESSIONAL PAPER 1288



CONTENTS

	Page
Abstract	1
Introduction	1
Previous investigations	2
Development of equations	4
Assumptions	4
Procedure	5
Calibration	8
Empirically developed relations	8
Calibration results	9
Sensitivity to assumed values of z	12
Applications	13
Channel adjustment	13
Width-discharge data from stable natural channels	17
Discussion	18
Conclusions	19
References cited	20
Appendix	21

ILLUSTRATIONS

	Page
FIGURE 1. Graph showing variation of normalized shear stress with proportional distance along half the perimeters of hypothetical alluvial channels	6
2. Graph showing variation of normalized maximum shear stress at the midline of a rectangular channel	7
3-12. Graphs showing width-discharge data and power relations for groups of channels:	
3. $W/D \leq 8.0$	10
4. $9.0 \leq W/D \leq 11.0$	10
5. $14.0 \leq W/D \leq 18.0$	10
6. $18.0 < W/D \leq 22.0$	10
7. $22.0 < W/D \leq 27.0$	10
8. $27.0 < W/D \leq 33.0$	10
9. $36.0 \leq W/D \leq 44.0$	11
10. $45.0 \leq W/D \leq 55.0$	11
11. $56.0 \leq W/D \leq 80.0$	11
12. $80.0 < W/D \leq 140$	11
13. Width-discharge relations for groups of stream channels with similar width-depth ratios	13
14. Graph showing the variation of the width exponent, b , with width-depth ratio	14
15. Graph showing change of b , f , m , z , and y with change of width-depth ratio	14
16. Graph showing change of b , f , m , and y , with variation in values of z for selected width-depth ratios	14
17-22. Graphs showing relations of width to discharge for channels of the Western United States:	
17. Graph showing relation of width to discharge for $14.0 \leq W/D \leq 18.0$	15
18. Graph showing relation of width to discharge for $18.0 < W/D \leq 22.0$	15
19. Graph showing relation of width to discharge for $22.0 < W/D \leq 27.0$	15
20. Graph showing relation of width to discharge for $27.0 < W/D \leq 33.0$	15
21. Graph showing relation of width to discharge for $36.0 \leq W/D \leq 44.0$	15
22. Graph showing relation of width to discharge for $45.0 \leq W/D \leq 55.0$	15

AN ANALYTICAL TREATMENT OF CHANNEL-MORPHOLOGY RELATIONS

By W. R. OSTERKAMP, L. J. LANE¹, and G. R. FOSTER¹

ABSTRACT

For a specified flow rate, the properties of channel width, mean depth, mean flow velocity, gradient, and roughness often are related to discharge by empirically developed power functions. Equations were derived that provide an analytical, or semitheoretical, basis for the empirical relations. The equations, which were calibrated and tested using field data, differ from previously derived power functions by incorporating variable exponents dependent on the shear-stress distribution along the channel section. Variable exponents permit the consideration of the entire range of natural channel geometries, including those of very wide braided channels that otherwise could not be described adequately by power functions. The derivation of these exponents is based on the continuity equation, the Manning equation, and an assumed equation for shear-stress distribution expressed in terms of channel width-depth ratio. By this approach, width-depth ratios are employed as surrogates for the channel sediment characteristics and the shear-stress distribution.

The equations were calibrated using channel data from the western half of the United States. The calibrated power equations were tested using data from relatively stable channels of the United States—in Ohio and southern Missouri—New Guinea, and Australia. Stable channels with steady discharge characteristics were selected for the testing to approximate the steady-state discharges assumed by the derivations. Results of the calibration and tests lead to generalizations concerning channel dynamics.

INTRODUCTION

The ancients observed that channels are molded by the water and sediment passing through them. In recent times attempts to quantify the channel changes that result from varying conditions of discharge have been made using concepts such as regime theory, hydraulic and channel geometry, and dynamic equilibrium.

Most efforts at quantification have been empirical and involve the use of power functions or similar simple equations to approximate the manner in which channel characteristics vary with discharge. The two sets of relations commonly developed in geomorphic studies have been (1) the variation of geometric and hydraulic variables (such as water surface or channel width and mean depth) with discharge or stage at a particular fixed channel cross section and (2) the variation of hydraulic (velocity, roughness) or geometric (width, depth, gradient) properties with discharge at different locations along a channel, measured on the basis of a common

hydraulic or geomorphic reference level. The first set of relations generally is termed the “at-a-station” case, and the second, to which attention is limited in this paper, is the “downstream” case (Leopold and Maddock, 1953, p. 4). The basic mathematics and assumptions on which the empirical studies depend are given in numerous papers on the topic and, therefore, are given here in summary form only. Many of the papers cited here, however, provide background explanations of the hydraulic- and channel-geometry methods.

This paper provides a semitheoretical basis for the use of power functions with variable exponents to describe the shapes of natural alluvial stream channels. Many of the empirical studies have defined the “downstream” changes of channel width, mean depth, and mean flow velocity as power functions of a discharge characteristic; the exponent values for each of the three power functions commonly have fallen in a limited range. As a result, approaches to definition of theoretical exponent values for the three power functions have concentrated on yielding single values representative of the limited range of values that the empirical studies typically provide. Variation in the exponent values for these empirical power functions does occur, however, and it cannot be reasonably assumed that single values of the exponents describe the range of conditions found in natural alluvial stream channels. The wide ranges of possible exponent values become apparent when the geometries of unusually wide or narrow channels are considered. Unlike previous theoretical or semitheoretical analyses of geometry-discharge relations, therefore, the present paper treats the entire range of geometries found in natural alluvial channels and proposes power functions with variable exponents partially based on theoretical considerations.

The mathematical approach of this paper is termed “analytical” instead of theoretical because the equations were developed, in part, from empirical relations and were calibrated using field data. The geometry data used for the calibration, collected from the western half of the United States, are summarized in an empirical study proposing variable geometry-discharge relations (Osterkamp and Hedman, 1982); this study is the basis

¹ U.S. Department of Agriculture

nels that are moderately cohesive, but empirical data, as well as theoretical considerations, suggest that use of single values leads to substantial error for channels formed of either highly cohesive or noncohesive material (Schumm, 1960; Knighton, 1974; and Williams, 1978).

The main purpose of this paper is to propose a derivation of the width, depth, and velocity exponents, b , f , and m , and to suggest that the value of each varies with the material forming the channel perimeter. The approach used in this paper extends the utility of several previous derivations by demonstrating that ranges of values for b , f , and m are justified on other than a purely empirical basis. Thus, the relations presented here can be used to anticipate the geometry resulting from specified conditions of water and sediment discharge or, conversely, for estimating discharge characteristics if channel conditions are known.

Substantial literature concerning the various power functions (eqs. 1-5) has accumulated. Most of the papers provide empirical evaluations of one or more of the exponents, but they are too numerous to provide a thorough discussion here. Among those that either are generally regarded as particularly significant or are especially pertinent to the present study are papers by Kennedy (1895), Lindley (1919), Lacey (1930), Lane (1937, 1957), Leopold and Maddock (1953), Wolman (1955), Blench (1957), Schumm (1960), Brush (1961), Hedman and Kastner (1977), Osterkamp (1978), and Osterkamp and Hedman (1982). A comprehensive list of references pertaining to hydraulic and channel geometry is presented by the Task Committee of the American Society of Civil Engineers (1982) on relations between morphology of small streams and sediment yields.

A variety of approaches has been used to replicate theoretically or semitheoretically the experimental geometry-discharge relations. Although the various methods use a wide range of equations and assumptions to define channel morphology, they all rely on the continuity equation ($Q = WDV$) and one or more additional relations to yield simultaneous solutions. Most approaches assume that the variables in the continuity equation can be expressed as power functions (eqs. 1-3). The assumption seems justified for the ranges of data normally considered, but is poorly founded for very small discharges (Osterkamp and Hedman, 1982). Use of the assumption, however, provides a second equation because the expansion of the continuity equation to power form requires that the sum of the exponents equal unity:

$$b + f + m = 1 \tag{6}$$

Table 1 provides comparisons of the theoretically developed power-function exponents (eqs. 1 to 5) pro-

TABLE 1.—Comparison of theoretically developed power-function exponents proposed by investigators

[Dashed entry means a value is not available; some values have been rounded to two significant figures]

Investigator	Width exponent b	Depth exponent f	Velocity exponent m	Gradient exponent z	Roughness exponent y
Leopold and Langbein (1962) _	0.55	0.36	0.09	-0.74	-0.22
Langbein (1964) _ _	.53	.37	.10	-.73	-.45
Tou Kuo-jen (1964) _	.56	.33	.11	----	----
Engelund and Hansen (1967) _ _	.52	.32	.16	-.21	----
Brebner and Wilson (1967) _ _ _	.47	.35	.18	-.12	----
Li Ruh-ming (1974)	.46	.46	.08	-.46	----
Smith (1974) _ _ _ _ _	.64	.27	.09	-.18	----
Parker (1979) _ _ _ _	.50	.42	.08	-.41	----
Lane and Foster (1980) ¹ _ _ _ _ _ _ _	.46	.46	.08	----	----

¹ Triangular cross section.

posed by Leopold and Langbein (1962), Langbein (1964), Tou Kuo-jen (1964), Engelund and Hansen (1967), Brebner and Wilson (1967), Li Ruh-ming (1974), Smith (1974), Parker (1979), and Lane and Foster (1980). In general, the values should be compared with caution because the assumptions, characteristic discharge, and type channel that led to the exponents are variable. Despite these problems, the values for b , the width exponent, range only from 0.46 to 0.64. The f and m values, for depth and velocity, derived from various theoretical approaches, also show relative consistency (table 1) and agree well with the majority of the empirically developed power functions. The values of z and y , for channel gradient and roughness, however, show substantial ranges in table 1. These exponents apparently are much more sensitive to the assumptions of a derivation, particularly the water- and sediment-flow characteristics used, than are the width, depth, and velocity exponents. A large range of empirical values for z , for example, has been reported. The smallest values, as low as 0.0, generally have been associated with low discharge rates, as represented by rill erosion (Lane and Foster, 1980) and controlled inflow in small channels (Ackers and Charlton, 1971). Values of z as great as -1.07 have been related to stable armored channels, such as Brandywine Creek in Pennsylvania, at the bankfull stage (Wolman, 1955, p. 26).

The basic form of a time-dependent model that recognizes channel morphology as the result of all discharges transmitted by the channel was presented by Pickup and Rieger (1979). Although this model does not provide specific derivations of geometry power functions, it is pertinent to the present analysis because the model proposes that channel size and shape are not unique to a dominant discharge. Pickup and Rieger suggested that channel geometry tends to fluctuate about a mean condi-

6. An equilibrium channel geometry (neither aggrading nor degrading) occurs when the shear stress at the lower corners of the rectangular channel section equals the critical shear stress for the given channel-bank material. It is assumed, therefore, that for specified conditions of discharge and particle sizes of channel material, an equilibrium condition signifies a specific width-depth ratio. By designating discharge and geometry (width-depth ratio), the need to consider explicitly particle sizes of channel material is eliminated.

All of the above assumptions were made, either implicitly or explicitly, in one or more of the theoretical investigations listed in table 1. For example, the assumption of power relations with discharge generally is made for the geometry variables (eqs. 1 to 5). Power relations describing shear-stress distributions also were assumed by Rohlf and Meadows (1980) and by Lane and Foster (1980), although the forms of equations differ from that assumed here (eq. 9). Rectangularly shaped channels commonly are considered when analyzing shear-stress data; these channels are assumed in the models of Brebner and Wilson (1967) and Lane and Foster (1980). Empirical flow-resistance equations or coefficients are incorporated into most of the derivations summarized by table 1.

PROCEDURE

The power-function derivations presented here, one for width and one for depth, involve four steps: (1) combining the continuity and Manning equations into a single equation involving both width and depth; (2) solving the assumed shear-stress distribution equation of a channel section for depth as a function of width (or vice versa); (3) substituting the result into the combined continuity-Manning relation to obtain a multiple power function for downstream changes of width or depth; and (4) substituting the required exponent values for the gradient and roughness power functions iteratively into the multiple power-function equations for width and depth until results consistent with empirical gradient relations and the Chézy equation are obtained. In other words, downstream equations for width and depth are developed as functions of the discharge, critical shear stress, gradient, and roughness at a channel section. To express the equations in the form of equations 1 and 2, all terms except that for discharge are included in the coefficient. Thus, in the end (eqs. 1 and 2), discharge remains as the sole independent variable, but its value depends on the input values for shear-stress distribution and the gradient and roughness exponents of equations 4 and 5.

Returning to the first step in greater detail, the discharge form of the Manning equation is simplified by

assuming that depth and hydraulic radius, R , of a channel section are nearly equal:

$$Q = \frac{\psi}{n} G^{1/2} W D^{5/3}. \quad (10)$$

The value of the constant ψ depends on the system of units used (for metric units, $\psi = 1.0$; in U.S. customary units, $\psi \approx 1.49$); other symbols are as previously defined. Rearranging gives

$$W^{3/5} D = \left[\frac{nQ}{\psi G^{1/2}} \right]^{3/5} \quad (11)$$

In order to consider shear-stress distribution in the channel section, an assumed distribution is solved in terms of width and depth and then combined with equation 11. An assumed rectangular channel has steady discharge, a width W , and a depth D . The wetted perimeter, P , is then $W + 2D$. Let x equal the distance from the water's edge to any point on the wetted perimeter up to the channel center. The proportional distance, x_* , along the wetted perimeter is the ratio of x , the distance along the wetted perimeter, to the length of the wetted perimeter:

$$x_* = x/P. \quad (12)$$

The proportional distance, x_* , thus ranges from 0 at the water's edge to 0.5 at the midline of the channel. The width-depth ratio of most natural stream channels exceeds 12, which permits the simplification that width nearly equals wetted perimeter.

The normalized shear stress, $\tau(x_*)/\bar{\tau}$, at any point along the wetted perimeter is a function of the proportional distance:

$$\tau(x_*)/\bar{\tau} = F(x_*). \quad (13)$$

If the function, $F(x_*)$ is assumed to be a power function:

$$\tau(x_*)/\bar{\tau} = p(x_*)^d, \quad (14)$$

where p is a coefficient, d is an exponent, and $0 < x_* \leq 0.5$.

In order to maintain a steady-state channel condition, the shear stresses along the banks must be less than, or equal to, the critical shear stress of the bank sediment, thereby assuring no bank erosion or channel widening. The shear stresses at points along the bed, however, must equal or exceed the critical shear stress for bed sediment in order that bed-load movement is maintained without causing aggradation. The transition between the cohesive material in the bank and the mobile particles on the bed occurs at the intersection of the vertical bank and the bed. At this point, which is equivalent to $x_* = D/W$, the shear developed by the flow equals the critical shear, τ_c , regardless of the character and mor-

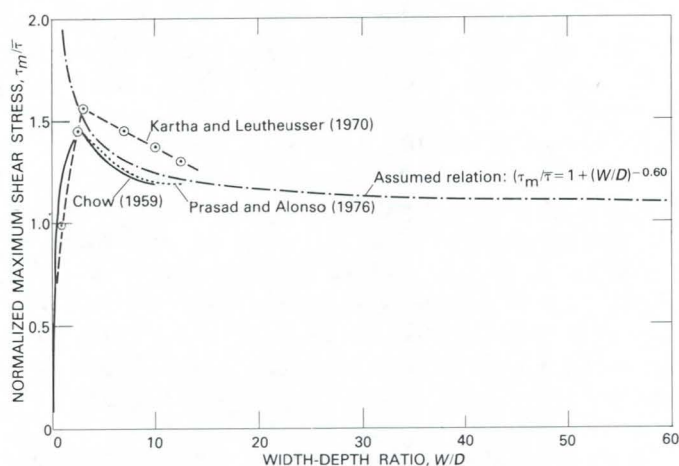


FIGURE 2.—Variation of normalized maximum shear stress at the mid-line of a rectangular channel, with width-depth ratio (W/D) for analytical and experimental data, and for the assumed relation $(\tau_m/\tau) = 1 + (W/D)^{-0.60}$.

Field data justifying equation 9 also have been published for channels with width-depth ratios exceeding 12.5. For example, some of Bathurst's (1979) normalized shear-stress data for gravel-lined natural channel sections compare favorably with the curves of figure 2. Because the Bathurst data were collected from natural channels that do not necessarily conform to the assumptions of this paper, the results are variable across channel sections and are not plotted in figure 2.

With increasing values of width-depth ratio above 3.0, the normalized maximum shear stress decreases asymptotically toward 1.0. With decreasing values of width-depth ratio below 3.0, the normalized maximum shear stress in other studies declines toward 0, whereas the assumed maximum shear stress in this paper approaches infinity. However, this portion of figure 2 is of minor consequence to the present discussion because the width-depth ratios of natural alluvial stream channels are usually much larger than 3.0 (for example, see data of Hedman and Kastner, 1977; and Osterkamp and Hedman, 1982). Thus, it is assumed that equation 9 leads to a reasonable description of the distribution of shear stresses across alluvial channels. From equations 9 and 22, it follows that

$$d = (W/D)^{-0.60}, \quad (23)$$

which is a necessary relation to solve equations 17 and 18. For the range of width-depth ratios expected in natural alluvial stream channels, values of d vary from nearly 0 to about 0.4, but values of d for most alluvial channels fall between 0.1 and 0.3 (corresponding to width-depth ratios of roughly 50 and 7, respectively).

In equations 17 and 18, ψ , p , γ , and τ_c can be incorporated into the coefficients a and c of equations 1 and 2. Gradient (G) and roughness (n), however, vary with

width-discharge and depth-discharge relations, and these variables must be considered when evaluating the exponents b and f . In other words, channel gradient and roughness are two of the five (eqs. 1 to 5) acknowledged degrees of freedom of self-adjusting channels (Williams, 1978, p. 2).

By defining coefficients a' and c' , respectively, equal to $\psi^{-j_1}(p\gamma)^{j_2}\tau_c^{-j_2}$ and $\psi^{-j_4}(p\gamma)^{-j_5}\tau_c^{j_5}$, equations 17 and 18 are simplified to

$$W = a'G^{j_3}n^{j_1}Q^{j_1} \quad (17a)$$

and

$$D = c'G^{-j_6}n^{j_4}Q^{j_4} \quad (18a)$$

By inserting the discharge terms for gradient and roughness from equations 4 and 5, simplifying and defining $a't^{j_3}r^{j_1}$ and $c't^{-j_6}r^{j_4}$, respectively, equal to a and c (eqs. 1 and 2), equations 17a and 18a are converted to

$$W = aQ^{(j_1+zj_3+vj_1)} \quad (24)$$

and

$$D = cQ^{(j_4-zj_6+vj_4)} \quad (25)$$

As suggested by the range of exponents shown in table 1, an accepted theoretical value for z is not available. Empirical data from relatively stable alluvial channels (having well-formed banks), however, indicate a value for z of -0.25 regardless of the particle-size characteristics of the material forming the channel perimeter (Lane, 1957; Osterkamp, 1978). This exponent is based on data from natural channels over wide ranges of mean discharge and gradient; the data were grouped according to similar characteristics of the channel material. For the downstream condition of stable channel sections formed of unchanging particle sizes, therefore, z does not vary significantly from -0.25 . Instead, from one channel to another, differences in the gradient-discharge relation (eq. 4), due to differences in the particle-size distribution, are reflected in the coefficient, t (Osterkamp, 1978). For very wide, braided channels, however, both theoretical considerations (for example, Leopold and Langbein, 1962, p. 12; Langbein, 1964, p. 309) and field evidence (Osterkamp and Hedman, 1982) suggest that z , as well as f , m , and y , must approach 0 as b approaches 1.0.

The bed-roughness exponent, y , is known, both from field investigations (Leopold and Maddock, 1953, p. 27; and Wolman, 1955, p. 27) and geometry relations (table 1), to be a generally small negative number when particle sizes of channel material do not change in the downstream direction. Although influenced by the width-depth ratio and its rate of change with discharge, increasing discharge in the downstream direction generally results in decreasing surface area of the channel per unit volume of discharge and stream length. In other words, discharge tends to increase in the downstream

evaluating the reasonableness of any assumed or calculated values of b and z .

To construct a curve relating the width exponent, b , to width-depth ratio, geometry and discharge data from several hundred gage sites of the western half of the United States (Osterkamp and others, 1982) were divided into 10 groups based on width-depth ratio; 318 channels were represented in groups: (1) $W/D \leq 8.0$, (2) $9.0 \leq W/D \leq 11.0$, (3) $14.0 \leq W/D \leq 18.0$, (4) $18.0 < W/D \leq 22.0$, (5) $22.0 < W/D \leq 27.0$, (6) $27.0 < W/D \leq 33.0$, (7) $36.0 \leq W/D \leq 44.0$, (8) $45.0 \leq W/D \leq 55.0$, (9) $56.0 \leq W/D \leq 80.0$, and (10) $80.0 < W/D \leq 140.0$.

Data for each group were plotted on logarithmic coordinates and a power relation was determined graphically using the data representing the narrowest channels relative to discharge (figs. 3 to 12). Although all available data were plotted, most are presumed indicative of channels widened to varying degrees by erosive flow events. The narrowest channels relative to discharge, therefore, are judged most representative of stable, fully adjusted conditions, and it is the data from these channels (except for several that appear to have been measured improperly) that most closely approximate the assumptions previously given. Thus, the linear relations of figures 3 to 12 are envelope curves (power functions), describing the narrowest naturally occurring channels for specified ranges of width-depth ratio. Where data are insufficient to describe with reasonable confidence the slope of a lower envelope relation, the slope is based, in large degree, on statistically developed relations from previous studies (Osterkamp, 1980; Osterkamp and Hedman, 1982).

CALIBRATION RESULTS

The results of figures 3 through 12 and the data upon which they are based are summarized by the equations listed in table 2 and the graphical comparison of them in figure 13. Comparison of the equations shows a nearly consistent increase of both coefficients and exponents with width-depth ratios.

The b exponents of the various width-discharge power functions (table 2; figs. 3 to 12) were plotted in figure 14 as a function of the mean value of width-depth ratio for each group. The plotted points are used to define a general curve (solid line) indicating the manner in which the b exponent for relatively stable alluvial stream channels varies with width-depth ratio. The solid line is extended as a dotted portion where data (table 2) are inadequate to provide reliable results. Also shown in figure 14 are similar points and a curve (dashed line) developed statistically from the width-discharge relations of Osterkamp and Hedman (1982) for groups of streams with similar channel-sediment characteristics.

In order that these data could be included and generalized in figure 14, mean values of width-depth ratio were determined for each channel-sediment group. Because several of the contrast groups show relatively large ranges of width-depth ratio, the mean values of width-depth ratio for the sediment groups (crosses, fig. 14) do not necessarily provide an accurate relation with the b exponents. The dashed-line curve nevertheless provides a comparison that supports the solid-line curve used here (fig. 14) through the low to moderate width-depth ratios; the dashed-line curve provides increased accuracy for the higher ratios. The displacement between the two curves probably is caused by the difference in method used to develop them. The solid-line curve is based on data representing only narrow, presumably stable, channel sections; the dashed-line curve is based on all data representing channel-sediment groups, many of which do not approach steady-state conditions.

The solid-line curve given in figure 14 is used as the principal basis of calibration for evaluating equations 24 and 25 because of (1) the similarity between it and the dashed-line curve of figure 14, (2) the general agreement of the b -values, taken from figure 14, with numerous other empirical values as well as most theoretically developed values (table 1), and (3) the solid-line curve's general conformity to the theoretical requirement that b approach 1.0 as width-depth ratios become very large. The b -exponent then corresponds to any width-depth ratio of the solid-line curve and is assumed accurate; the other four exponents (eqs. 2 to 5) are calculated accordingly.

Listed in table 3 for selected width-depth ratios of 5.0 to 1,000 are exponent values (for eqs. 1 to 5) and the d and j values from which they were calculated. The b values, taken directly from the curve of figure 14, are those values corresponding to the selected width-depth ratios. Also listed are values of j_2 and j_5 that are necessary to calculate the coefficients of equations 24 and 25. The exponents are given to three significant figures in order to provide consistency, but there is no

TABLE 2.—Power relations of width to discharge developed from field data of channels in the Western United States and grouped by width-depth ratios

[W, channel width in meters; Q, mean discharge in cubic meters per second]				
Width-depth ratios				
Group	Figure No.	Range	Midpoint	Equation
1	3	≤ 8.0	7.0	$W = 4.1Q^{0.48}$
2	4	9.0–11.0	10.0	$W = 4.6Q^{0.49}$
3	5	14.0–18.0	16.0	$W = 4.8Q^{0.51}$
4	6	>18.0–22.0	20.0	$W = 5.8Q^{0.54}$
5	7	>22.0–27.0	24.5	$W = 5.8Q^{0.51}$
6	8	>27.0–33.0	30.0	$W = 6.4Q^{0.53}$
7	9	36.0–44.0	40.0	$W = 6.6Q^{0.56}$
8	10	45.0–55.0	50.0	$W = 6.9Q^{0.58}$
9	11	56.0–80.0	68.0	$W = 6.0Q^{0.77}$
10	12	>80.0–140	110	$W = 7.1Q^{0.82}$

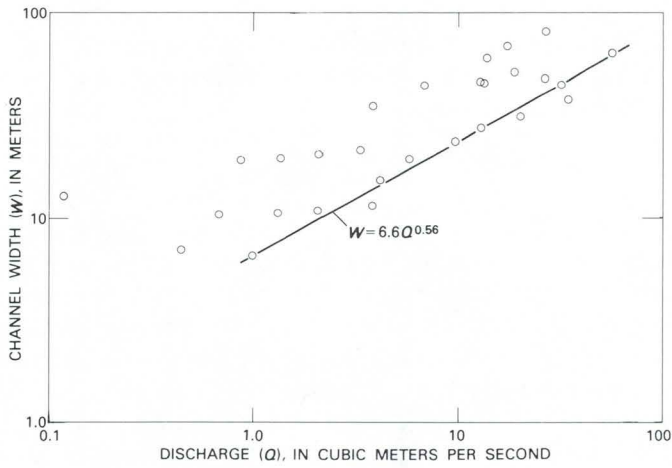


FIGURE 9. $-36.0 \leq W/D \leq 44.0$.

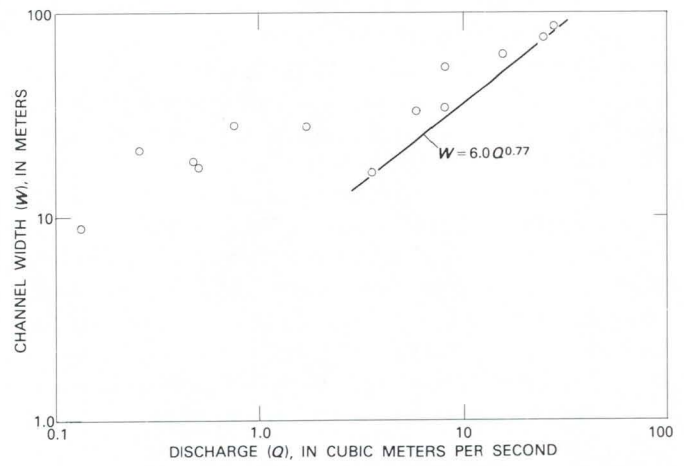


FIGURE 11. $-56.0 \leq W/D \leq 80.0$.

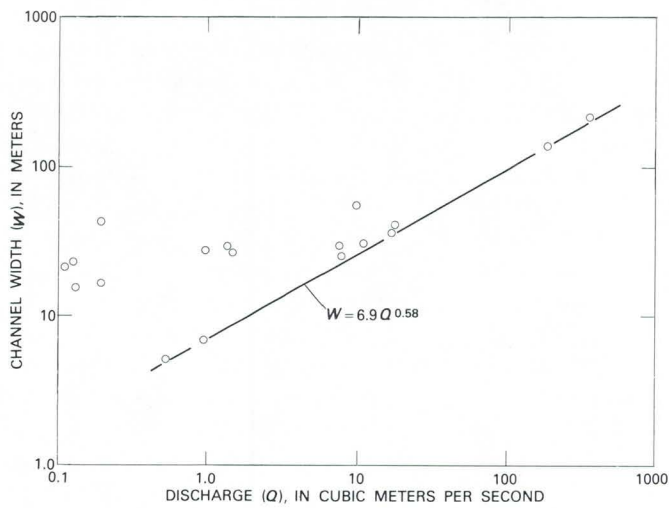


FIGURE 10. $-45.0 \leq W/D \leq 55.0$.

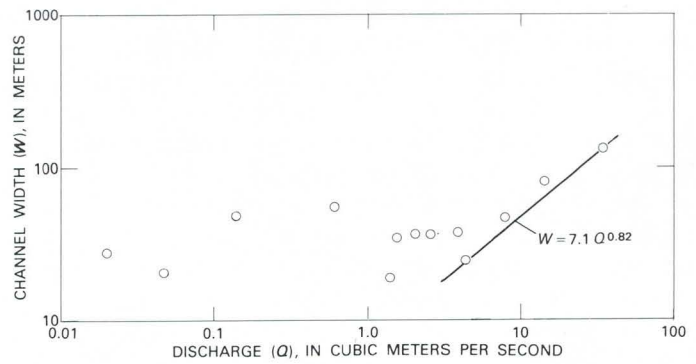


FIGURE 12. $-80.0 \leq W/D \leq 140$.

data points representing the narrowest reliable width measurements, relative to mean discharge, that are available.

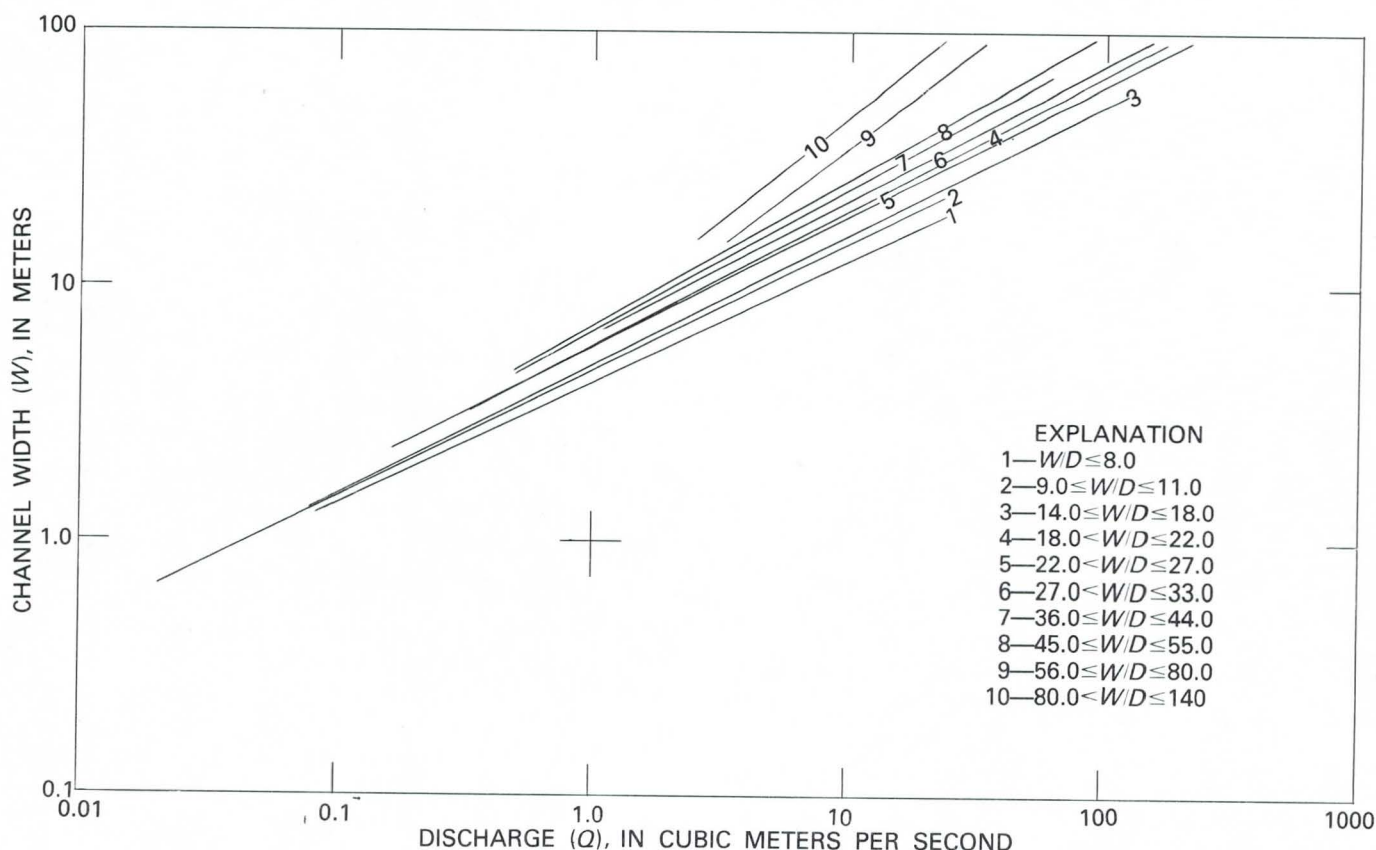


FIGURE 13.—Width-discharge relations for groups of stream channels with similar width-depth ratios (W/D).

downstream direction, the z -exponent (eq. 4) normally varies between -0.25 and -0.40 . However, lower negative values occur for very wide stream channels relative to discharge (table 2).

Figure 16 also illustrates that the b , f , m , and y exponents show increasing sensitivity to changes in z with increasing width-depth ratio. The f and y exponents, for depth and bed roughness, show the greatest rates of change with variation of z , but the absolute effect on any y -value by changes of z is minor owing to the small magnitude of y . The width exponent, b , shows limited change with z values of smaller magnitude than -0.4 ; this suggests that, as pointed out earlier, of the five exponents (eqs. 1 to 5), b is well-suited to be the basis for calibrating equations 24 and 25.

APPLICATIONS

Equations 24 and 25, which are semitheoretical, and the equations of table 2, which provide both empirical support and a means of calibrating equations 24 and 25, demonstrate that geometry-discharge relations of alluvial channels cannot be readily generalized from single power equations. The recognition that the coeffi-

cients and exponents of equations 1 to 5 are variable, dependent at least in part on the mobile sediment supply of a channel system, leads to various assumptions and conclusions regarding fluvial processes. Several of these assumptions and conclusions are discussed in the following section.

CHANNEL ADJUSTMENT

Basic to the derivation leading to equations 24 and 25 is that the mean shear stress in a channel is a function of the instantaneous water-sediment discharge:

$$\bar{\tau} = F(Q_i). \quad (28)$$

Among the assumptions of the derivation is the occurrence of approximate channel adjustment to the mean-discharge conditions of the water-sediment mixture. As discharge in a channel section increases, the erosiveness (owing to greater velocities and turbulence) generally increases also. Thus, the assumption of equilibrium requires relatively uniform discharge conditions in which the erosive (shear) stresses at the channel perimeter are in balance through time with the gravitational and cohesive forces resisting movement of channel sediment.

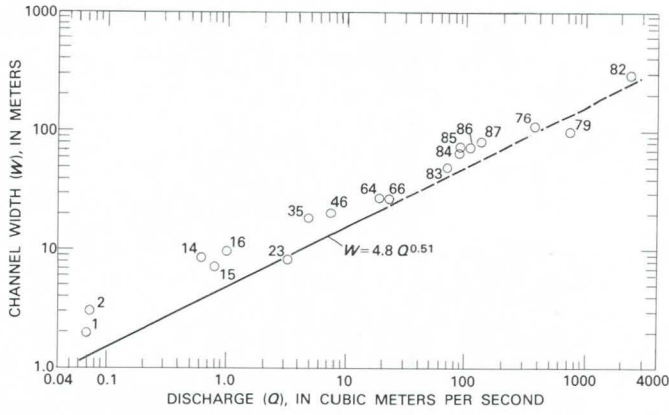


FIGURE 17.—Relation of width to discharge for $14.0 \leq W/D \leq 18.0$.

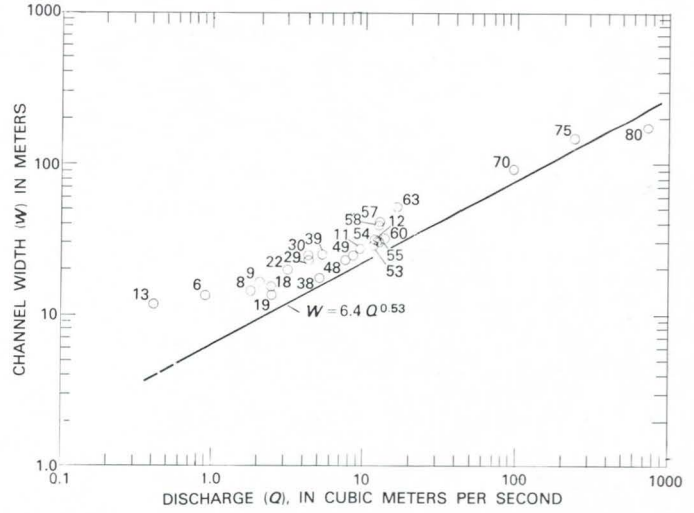


FIGURE 20.—Relation of width to discharge for $27.0 < W/D \leq 33.0$.

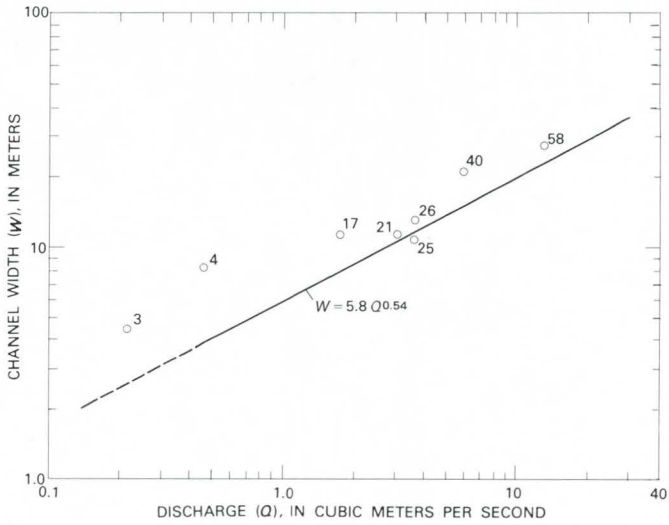


FIGURE 18.—Relation of width to discharge for $18.0 \leq W/D \leq 22.0$.

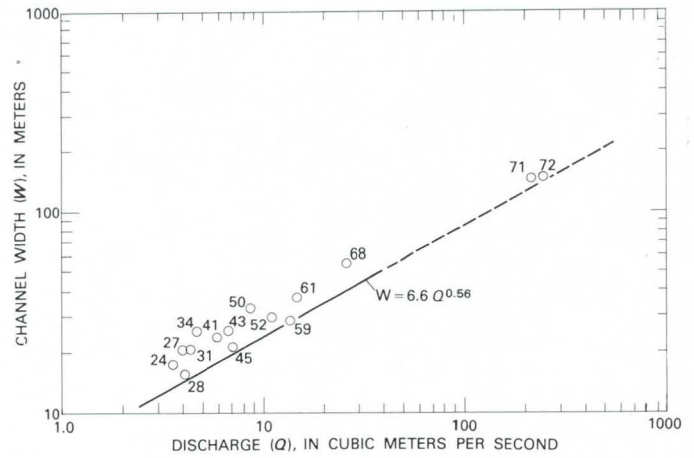


FIGURE 21.—Relation of width to discharge for $36.0 \leq W/D \leq 44.0$.

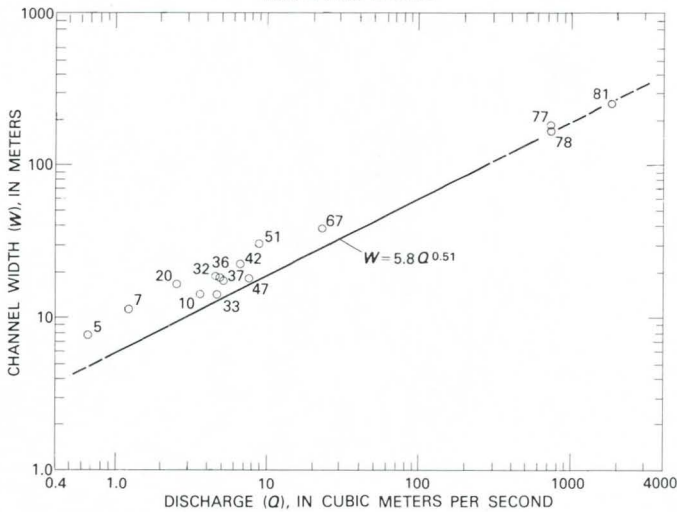


FIGURE 19.—Relation of width to discharge for $22.0 < W/D \leq 27.0$.

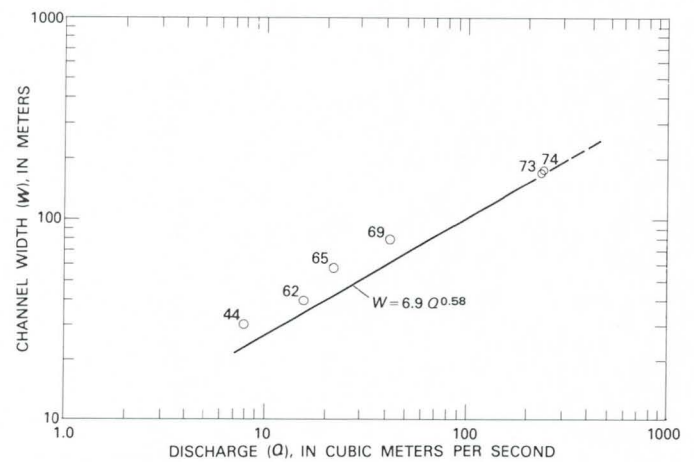


FIGURE 22.—Relation of width to discharge for $45.0 \leq W/D \leq 55.0$.

FIGURES 17-22.—Relations of width to discharge for channels of the Western United States. Numbers refer to comparative data in table 4 from the United States—in Ohio and southern Missouri—New Guinea, and Australia; dashed segments are extrapolations of the relation lines beyond the limits defined by the Western United States data.

TABLE 4.—Geometry-discharge data from natural stream channels with stable discharge—Continued

Stream and location	Data-set No.; Fig. No. ¹	Width in meters	Mean depth in meters	Width-depth ratio	Mean discharge in cubic meters per second	Source of data ²	Comments
Little Miami River near Spring Valley, Ohio	52;23	30.2	.732	41.3	10.9	2	
Killbuck Creek at Killbuck, Ohio	53;22	29.0	.945	30.7	11.5	2	
Cuyahoga River at Old Portage, Ohio	54;22	31.1	1.01	30.8	11.9	2	
Tuscarawas River at Missillon, Ohio	55;22	29.9	1.07	27.9	12.3	2	
Big Darby Creek at Darbyville, Ohio	56;22	39.0	1.31	29.8	12.7	2	
Scioto River near Prospect, Ohio	57;22	40.8	1.49	27.4	12.8	2	
Hocking River at Enterprise, Ohio	58;20	27.7	1.34	20.7	12.9	2	
Great Miami River at Sidney, Ohio	59;23	29.0	.671	43.2	13.4	2	
Mad River near Springfield, Ohio	60;22	32.3	1.19	27.1	13.7	2	
Little Beaver Creek near East Liverpool, Ohio	61;23	38.4	1.01	38.0	14.7	2	
East Fork Little Miami River at Perintown, Ohio	62;24	39.3	.792	49.6	15.6	2	
Licking River near Newark, Ohio	63;22	51.5	1.71	30.1	16.4	2	
Raccoon Creek at Adamsville, Ohio	64;19	27.7	1.62	17.1	18.5	2	
Scioto River near Dublin, Ohio	65;24	57.0	1.19	47.9	22.2	2	Below O'Shaughnessy Dam, regulated
Cuyahoga River at Independence, Ohio	66;19	27.4	1.52	18.0	22.7	2	
Paint Creek near Bourneville, Ohio	67;21	39.0	1.55	25.2	22.7	2	
Mohican River at Greer, Ohio	68;23	55.5	1.31	42.4	25.5	2	
Walhonding River near Nellie, Ohio	69;24	79.6	1.65	48.2	41.6	2	Below Mohawk Dam, regulated
Scioto River at Chillicothe, Ohio	70;22	92.0	2.80	32.9	96.5	2	
Muskingum River at McConnellsville, Ohio	71;23	151	3.84	39.3	211	2	
Ok Tedi at Ningerum, New Guinea, sec. 1	72;23	150	3.5	42.9	240	3	Gage site
Ok Tedi at Ningerum, New Guinea, sec. 2	73;24	170	3.5	48.6	240	3	1030 m upstream of gage
Ok Tedi at Ningerum, New Guinea, sec. 3	74;24	175	3.5	50.0	240	3	2250 m upstream of gage
Ok Tedi at Ningerum, New Guinea, sec. 4	75;22	150	5.0	30.0	240	3	3310 m upstream of gage
Aure River near mouth, New Guinea	76;19	110	7.5	14.7	370	3	
Alice River at Kokonda, New Guinea, sec. 1	77;21	185	7.0	26.4	726	3	4190 m downstream of gage
Alice River at Kokonda, New Guinea, sec. 2	78;21	170	7.5	22.7	726	3	2100 m downstream of gage
Alice River at Kokonda, New Guinea, sec. 3	79;19	100	6.0	16.7	726	3	Gage site
Alice River at Kokonda, New Guinea, sec. 4	80;22	175	6.0	29.2	726	3	2460 m upstream of gage
Fly River at Kuambit, New Guinea	81;21	260	9.9	26.3	1780	3	
Purari River below Wabo Dam site, New Guinea	82;19	250	14.3	17.5	2360	3	Width average of three sections; depth estimated
Murrumbidgee River near Maude, Australia	83;19	50.3	3.6	14.0	68.5	4	Depth estimated
Murrumbidgee River near Darlington Point, Australia	84;19	67.1	4.0	16.7	86.6	4	Do.
Murrumbidgee River near Hay, Australia	85;19	74.7	5.3	14.1	88.5	4	Do.
Murrumbidgee River near Narrandera, Australia	86;19	75.0	4.5	16.7	104	4	Do.
Murrumbidgee River near Wagga Wagga, Australia	87;19	83.2	5.0	16.6	130	4	Do.

¹ First number is data number shown on the appropriate figure (graph), which is given by the second number 2.

² 1, Field investigations, W. R. Osterkamp; 2, E. E. Webber, written commun. 1981; Webber and Roberts, 1981; 3, Pickup (1977) and Pickup and others (1979); 4, Schumm (1968).

rapid—within a few years if erosive floods do not occur in that period (Osterkamp and Harrold, 1982).

WIDTH-DISCHARGE DATA FROM STABLE NATURAL CHANNELS

Because hydrologic conditions of the Western United States may be generally conducive to wide and poorly adjusted channel conditions, the relation lines of figures

3 to 12 were tested further using data from natural channels with relatively stable discharge (channels with low flood peaks relative to mean discharge). These data include widths, depths, and mean discharges from (1) spring-effluent channels of southern Missouri, (2) various-sized streams of Ohio (Webber and Roberts, 1981; E. E. Webber, written commun., 1981), (3) large streams of southwestern New Guinea, an area of tropical rainforest (Pickup, 1977; Pickup, and others,

justs its geometry to accommodate (1) the water and sediment discharges, (2) the gradient constraints imposed by topography, and (3) the fabric strength of the channel alluvium. In the derivation summarized by equations 28 and 29, these changes are viewed not simply as an adjustment of geometry to imposed conditions of shear stress, but also as an adjustment of shear stresses, at the wetted perimeter, toward a limited range that prevails for all stable alluvial channels. As indicated by figure 1 and subject to the assumptions of this paper, the shear stresses near the edges of a rectangular channel section rapidly approach 0 regardless of the width-depth ratio. This means that the distribution of shear stresses tends to be similar along the wetted perimeters of all stable alluvial channels that approximate the rectangular shape assumed, in this paper, for a condition of constant discharge. Variation in width-depth ratio, which appears to be dependent on the sizes and sorting of the sediment supply, serves to adjust the maximum shear stress and water velocity in parts of the channel sections other than the wetted perimeter. This conclusion is supported indirectly by data showing that fluvial-sorting processes of bank material in most relatively stable alluvial channels result in particle-size distributions that are largely independent of the size, shape, or gradient of the channels (Osterkamp, 1981; Osterkamp and Harold, 1982).

In summary, the derivation of this paper is based on width-depth ratios that imply specific shear-stress distributions. Dependent on the sediment-discharge characteristics and topographic constraints, the channel gradient and roughness adjust to produce water velocities and turbulence that maintain the requirement of sediment mass balance. For example, a wide range of channel gradients was found for channels with width-depth ratios of 20 (Osterkamp and others, 1982). The streams of high gradient are very turbulent owing to armoring and high channel roughness, whereas those of low gradient are commonly sand- or gravel-bedded channels. Both types are assumed adjusted to flow rates roughly approximating mean discharge, although the armor of the steep channels is moved only during relatively high flows. However, should large sediment sizes become unavailable for transport by the high-gradient stream, continued armoring is not possible. The necessary adjustment to maintain sediment mass balance then would be channel widening, an increase of the width-depth ratio, and a reduction of the maximum shear stress (fig. 1).

CONCLUSIONS

The derivation of the width and depth exponents in equations 24 and 25 is based on the continuity equation,

the Manning equation, and an assumed relation describing the approximate manner in which shear-stress distributions of stable alluvial channels vary with channel geometry. The shapes of alluvial channels, however, are closely related to the sediment transported by streams and stored as material forming the bed and banks. Thus, the analytical approach of this paper indirectly considers the characteristics of channel sediment as an independent variable determining the downstream changes of channel morphology relative to water discharge. Unlike previous approaches that relate downstream changes in geometry and discharge as power functions with fixed exponents, the approach presented here results in variable power-function exponents (equations 1 to 5) that necessarily vary with the shape (and, therefore, also with the sediment characteristics) of alluvial channels.

Weaknesses of the approach described here include the assumptions necessary for the derivation of the exponents, such as a condition of constant discharge and a rectangular channel shape, and the need for iterative calibration by use of field data. Despite the weaknesses, however, the derived equations in this paper appear to relate the geometries of alluvial channels reasonably well to the mean discharges typical of those channels. The equations appear applicable to the entire range of natural alluvial channels, including those that are unusually wide or narrow relative to depth. The equations probably are not applicable to channels of ephemeral and intermittent streams or to channels that are not fully fluvial, such as those modified by tidal effects.

Although the assumptions necessary to the derivation of the exponents limit its application to natural stream channels, the forms of the equations derived in this paper are useful for understanding channel dynamics. Equation 17, for example, is based in part on the Manning equation, but perhaps it explains channel adjustments more effectively than the Manning equation. Because steady-state conditions are assumed, equation 17 shows that a change in any one of the variables must result in adjustment by one or more of the other variables in order to reach a balanced channel condition. The equation suggests that the balance between geometry and discharge necessary to maintain stable channel conditions is the result of a similar balance between the distribution of shear stresses along the channel perimeter and the channel properties.

Equation 17, therefore, suggests that if, at constant discharge and roughness, the gradient of a channel is increased, a likely result is some combination of increased width and critical shear stress. Conversely, as a channel reach develops smaller and smaller gradients through

Osterkamp, W. R., Hedman, E. R., and Wiseman, A. G., 1982, Geometry, basin-characteristic, discharge, and particle-size data from gaged stream-channel sites of the western United States: U.S. Geological Survey Hydrologic Data Open-File Report 82-93, 56 p.

Parker, Gary, 1979, Hydraulic geometry of active gravel rivers: American Society of Civil Engineers, Journal of the Hydraulics Division, HY9, p. 1185-1201.

Pickup, G., 1977, Computer simulation of the impact of the Wabo Hydroelectric Scheme on the sediment balance of the lower Purari: Purari River (Wabo) Hydroelectric Scheme Environmental Studies, v. 2, Office of Environment and Conservation, Papua, New Guinea.

Pickup, G., Higgins, R. J., and Warner, R. F., 1979, Impact of waste rock disposal from the proposed Ok Tedi mine on sedimentation processes in the Fly River and its tributaries: Department of Minerals and Energy, Papua, New Guinea.

Pickup, G., and Rieger, W. A., 1979, A conceptual model of the relationship between channel characteristics and discharge: Earth Surface Processes, v. 4, p. 37-42.

Prasad, S. N., and Alonso, C. V., 1976, Integral-equation analysis of flows over eroding beds: Proceedings, American Society of Civil Engineers Symposium on Inland Waterways for Navigation, Flood Control, and Water Divisions, Fort Collins, Colorado, v. 1, p. 760-772.

Replogle, J. A., and Chow, V. T., 1966, Tractive-force distribution in open channels: Journal of the Hydraulics Division, American Society of Civil Engineers, HY7, p. 169-189.

Rohlf, R. A., and Meadows, M. E., 1980, Dynamic mathematical modeling of rill erosion: Proceedings, American Society of Civil Engineers Symposium on Watershed Management, Boise, Idaho, v. 1, p. 13-26.

Schumm, S. A., 1960, The shape of alluvial channels in relation to sediment type: U.S. Geological Survey Professional Paper 352-B, 30 p.

——— 1968, River adjustment to altered hydrologic regimen—Murrumbidgee River paleochannels, Australia: U.S. Geological Survey Professional Paper 598, 65 p.

Schumm, S. A., and Lichty, R. W., 1963, Channel widening and floodplain construction along Cimarron River in southwestern Kansas: U.S. Geological Survey Professional Paper 352-D, p. 71-88.

Smith, T. R., 1974, A derivation of the hydraulic geometry of steady-state channels from conservation principles and sediment transport laws: Journal of Geology, v. 82, p. 98-104.

Task Committee of the American Society of Civil Engineers, 1982, Relations between morphology of small streams and sediment yield: Journal of the Hydraulics Division, American Society of Civil Engineers, HY11, p. 1328-1365.

Tou Kuo-jeu, 1964, Hydromorphology of alluvial channels of lowland rivers and tidal estuaries [English translation from Naval Oceanographic Office, Washington, D.C.]: Shuili Hwei Pao, no. 2, 23 p.

Trask, P. D., 1959, Effect of grain size on strength of mixtures of clay, sand, and water: Geological Society of America Bulletin, v. 70, p. 569-579.

Webber, E. E., and Roberts, J. M., 1981, Flood-flow characteristics related to channel geometry in Ohio: U.S. Geological Survey Open-File Report 81-1105, 28 p.

Williams, G. P., 1978, Hydraulic geometry of river cross sections—theory of minimum variance: U.S. Geological Survey Professional Paper 1029, 47 p.

Wolman, M. G., 1955, The natural channel of Brandywine Creek, Pennsylvania: U.S. Geological Survey Professional Paper 271, 50 p.

Wolman, M. G., and Brush, L. M., Jr., 1961, Factors controlling the size and shape of stream channels in coarse noncohesive sands: U.S. Geological Survey Professional Paper 282-G, p. 183-210.

APPENDIX

[List of numbered equations provided in the text]

Equation number	Equation	Page
1.	$W = aQ^b$ -----	2
2.	$D = cQ^f$ -----	2
3.	$V = kQ^m$ -----	2
4.	$G = tQ^z$ -----	2
5.	$n = rQ^y$ -----	2
6.	$b + f + m = 1$ -----	3
7.	$Q_i = WDV$ -----	4
8.	$Q_i = k'Q_i^b Q_i^f Q_i^m$ -----	4
9.	$\tau_m/\bar{\tau} = 1 + (W/D)^{-0.60}$ -----	4
10.	$Q = -\frac{\psi}{n} G^{1/2} W D^{5/3}$ -----	5
11.	$W^{3/5} D = \left[\frac{nQ}{\psi G^{1/2}} \right]^{3/5}$ -----	5
12.	$x_* = x/P$ -----	5
13.	$\tau(x_*)/\bar{\tau} = F(x_*)$ -----	5
14.	$\tau(x_*)/\bar{\tau} = p(x_*)^d$ -----	5
15.	$\tau_c/\gamma GD = p(D/W)^d$ -----	6
16.	$W = \left[\frac{\gamma G p}{\tau_c} \right]^{(5/8d+3)} \left[\frac{nQ}{\psi G^{1/2}} \right]^{(3d+3/8d+3)}$ -----	6
17.	$W = \psi^{-j_1} (p\gamma)^{j_2} \tau_c^{-j_2} G^{j_3} n^{j_1} Q^{j_1}$ -----	6
17a.	$W = a' G^{j_3} n^{j_1} Q^{j_1}$ -----	7
18.	$D = \psi^{-j_4} (p\gamma)^{-j_5} \tau_c^{j_5} G^{-j_6} n^{j_4} Q^{j_4}$ -----	6
18a.	$D = c' G^{-j_6} n^{j_4} Q^{j_4}$ -----	7
19.	$\bar{\tau} = \frac{1}{0.5} \int_0^{0.5} \tau(x_*) dx_*$ -----	6
20.	$p = 2^d(d+1)$ -----	6
21.	$(\tau_m/\bar{\tau}) = p(0.5)^d$ -----	6
22.	$d = (\tau_m/\bar{\tau}) - 1.0$ -----	6
23.	$d = (W/D)^{-0.60}$ -----	7
24.	$W = aQ^{(j_1+j_3+j_4)}$ -----	7
25.	$D = cQ^{(j_4-j_2-j_6+j_4)}$ -----	7
26.	$C \sim \frac{R^{0.167}}{n}$ -----	8
27.	$y = -0.167f$ -----	8
28.	$\bar{\tau} = F(Q_i)$ -----	13
29.	$[W, D, G, n, d_{50}, SC, \dots]^{1/2} F(Q_i)$ -----	14